Journal of Sound and Vibration (2003) **259**(5), 1067–1079
doi:10.1006/jsvi.2002.5131, available online at http://www.idealibrary.com on IDEAL®

THE SOUND FIELD OF A ROTOR IN A STATIONARY DUCT

M. Carley

Department of Mechanical Engineering, University of Bath, Bath BA2 7AY, England, UK

(*Received* 26 *November* 2001, *and in final form* 11 *February* 2002)

A method is developed for the prediction of noise from rotors in an axisymmetric duct at rest. The technique combines a previously developed model for noise from disc sources with a boundary integral equation method for scattering from the duct surface. Recent developments in the theory of Gaussian quadrature and generalized elliptic integrals are used to simplify the implementation of the formulation. The sound field of a simplified model ducted rotor is then calculated and its structure examined in the framework of known features of the field around rotating sources. It is found that, as for an open rotor, the sonic radius plays an important role in the structure of the field.

1. INTRODUCTION

One of the most striking features of modern aircraft compared to earlier designs is their comparatively low noise level. A recent survey of trends in aircraft performance and operating characteristics [1] shows that average take-off noise levels for commercial jet aircraft have fallen by 25 dB in 30 years. To some degree this reduction has been brought about by stricter regulations forcing airlines to operate, and manufacturers to build, quieter aircraft but it has only been made possible by the improved understanding of aerodynamic noise generation processes. In particular, models based on the work of Lighthill [2] have led to large reductions in jet exhaust noise: the comparatively low noise generated by modern high bypass engines is a striking example of the eighth power law in action. The reduction of jet noise and the move towards physically larger engines have, however, caused new problems. As jet noise is reduced, the tonal noise generated by the fan becomes subjectively more important and, being tonal, makes the engine noise more annoying, a point noted in the early study of Tyler and Sofrin [3]. Furthermore, in modern engines the tonal noise is louder because of the larger fan and the larger intake from which noise radiates. This has led to greater interest in the problem of noise propagation in, and radiation from, ducts.

2. DUCTED FAN NOISE

The calculation of noise radiated by ducted fans is a problem in source modelling and in acoustic scattering. In this work, the source will be modelled as a disc using the methods of previous studies of the structure of rotating sound fields [4, 5]. This allows the accurate calculation of the sound field of a rotating source even very close to the disc, an essential point given the small tip clearances typical of ducted fans. Since the acoustic field of a disc source has features not seen on ring sources, the use of a realistic source model is important in predicting the acoustic field.

0022-460X/02/$35.00

The field scattered by the duct is calculated using a Helmholtz boundary integral equation. This is solved by using a boundary element method employing recent advances in numerical quadrature of singular functions and in the theory of generalized elliptic integrals, which are used to represent the singular part of the Green function in axisymmetric problems. The resulting numerical method is efficient, accurate and capable of being adapted to use advanced solution techniques such as that of Burton and Miller [6].

2.1. SOUND FROM DUCTED SOURCES

The problem of noise radiation from ducted rotors can be viewed as a problem in duct acoustics or as a scattering problem. Much of the physical insight into propagation in, and radiation from, ducts has come from "duct acoustics" models where the wave equation is solved subject to a boundary condition imposed on the duct wall and with the implicit assumption that the duct is long, i.e., infinite or semi-infinite. By using such an approach it has been possible to solve analytically realistic problems which demonstrate the behaviour of waves propagating in ducts. The sound field in a duct is composed of a sum of modes which have, in a circular duct, sinusoidal azimuthal variation and a Bessel function radial variation. At a given frequency ω, the acoustic pressure p in a circular duct of radius R is made up of modes of the form [7]

$$p(r, z, \theta, t) = P_{mn} e^{-j\omega t} J_m(k_{mn} r) e^{j(k_{z_{mn}} z \pm m\theta)},$$

where m is an integer, J_m is a Bessel function of order m, k_{mn} is the nth solution of

$$J'_m(k_{mn} R) = 0$$

and the axial wavenumber $k_{z_{mn}}$ is given by

$$k^2_{z_{mn}} = k^2 - k^2_{mn},$$

where the temporal wavenumber $k = \omega/c$. When $k < k_{mn}$, $k_{z_{mn}}$ is imaginary so that the corresponding mode decays exponentially in the duct and is said to be "cut off". When the duct radius varies axially, the eigenvalues k_{mn} also vary and modes can be cut off in some parts of the duct, but not in others [8] so that the duct acts as a filter. The field inside the duct depends on the source, which generates the modes, and the duct termination conditions, which specify how the field inside the duct is coupled to the radiated field outside. The number of modes which are "cut on" (propagate) will depend, for a given azimuthal order m, on the frequency of the source. For each mode, there is a cut-off frequency and the source frequency must exceed this value, if a mode is to propagate. This frequency ω can be non-dimensionalized on the speed of sound c and the duct radius R, yielding a Mach number $M = \omega R/c$, which is the non-dimensional velocity at which the azimuthally varying pressure pattern sweeps the duct wall. In order to propagate, an acoustic mode must have a frequency higher than cut-off or, equivalently, a Mach number higher than the cut-off value.

2.2. ROTATING SOUND FIELDS

The sound field radiated by rotating sources is a complex and rich one, especially at high frequency. The structure of such fields has been studied by using a variety of approaches which agree on the fundamental features. In a number of papers on the physical structure of such acoustic fields [4, 5, 9, 10], it has been shown that the field is characterized by the sonic radius r of the rotating source. This is the distance from the axis of rotation at which

the source has, or would have, sonic velocity relative to the fluid. For a stationary source rotating at angular velocity Ω, $r = c/\Omega$. The sonic radius marks the division of the acoustic field between the near field and the far field or radiation zone. In the near field, acoustic energy spirals around the axis many times before escaping into the far field across a transition region of thickness equal to roughly half an acoustic wavelength. In "tunnelling" across this transition region, there is an exponential decay in the acoustic energy [10] so that the radiation in the far field is usually quite weak. The exception to this is the field of a supersonic rotor. In this case, part of the source lies outside the sonic radius and no energy is lost in tunnelling across the transition region. From reciprocity considerations [11], it is obvious that the acoustic field must decay across the transition region in either direction.

The objective of the numerical study presented in section 4 is to examine the effect of different fan speeds in terms of the position of the sonic radius relative to the surrounding duct.

2.3. COMPUTATIONAL METHODS

The calculation of noise radiated by ducted sources is presently best performed by using the finite element method [7]. The technique has a number of advantages over finite difference and boundary integral approaches which make it the method of choice for realistic problems, especially in calculating noise from aeroengine intakes. These advantages include the treatment of sound propagation in non-uniform mean flows and the ability to handle complex geometries. There are certain difficulties which must be overcome, however, including the imposition of a physically correct radiation boundary condition at the edge of the computational domain. There also remains the problem that a large part of the domain must be meshed, which can be computationally intensive at high frequency. That said, the problem of the radiation boundary condition has been largely solved and many of the difficulties which arise in applying the finite element method to realistic problems would also arise in any other approach to the radiation problem.

For the simplified problem treated in this paper, however, a boundary element method has been adopted. The reasons for this include the lower dimensionality of the problem, making its implementation simpler, and the requirement to calculate the acoustic field only at points of interest, rather than over some computational domain. As yet, a boundary integral method capable of solving problems of the same complexity as those covered by the finite element approach does not exist but a number of steps have been made towards greater realism. In particular, the recent work of Dunn *et al.* [12] has led to a method capable of solving for scattering by straight, infinitesimal wall-thickness ducts in a mean flow, including the effects of an acoustic liner. The method presented in this paper does not include the effect of a mean flow but does allow a more general geometry to be modelled.

3. FORMULATION

The problem to be solved is that of calculating the field scattered by a hard-walled axisymmetric body subject to an incident field from a disc source. This can be done using a Helmholtz integral equation solved using a boundary element method. The incident fan field is calculated using an approach derived in previous work [4] which allows the acoustic field to be accurately calculated in the near field, essential in a realistic model for ducted fan noise, where tip clearances are typically small.

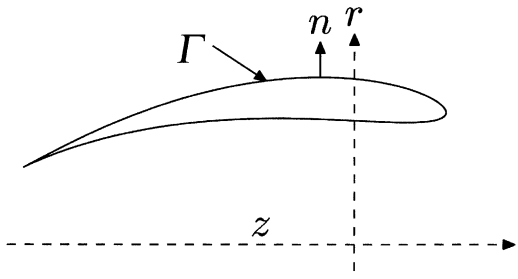

Figure 1. Geometry definition.

The duct geometry is shown in Figure 1. The duct is axisymmetric and formed by the rotation of a generating curve Γ about the z-axis. Cylindrical co-ordinates (r, θ, z) are used. The outward pointing surface normal is denoted by $\mathbf{n}$. The boundary integral equation for the surface pressure is that given by Wu and Lee [13],

$$C(\mathbf{x})P(\mathbf{x}) = \int_A G\frac{\partial P}{\partial \mathbf{n}_1} - P\frac{\partial G}{\partial \mathbf{n}_1}\,\mathrm{d}A \tag{1}$$

with

$$C(\mathbf{x}) = 1 + \int_A \frac{\partial G_0}{\partial \mathbf{n}_1}\,\mathrm{d}A.$$

The body surface is A, P is pressure at frequency ω and G is the free space Green function,

$$G = \frac{\mathrm{e}^{\mathrm{j}kR}}{4\pi R}, \qquad R = [r^2 + r_1^2 - 2rr_1\cos\theta_1 + (z - z_1)^2]^{1/2}, \tag{2}$$

where the wavenumber $k = \omega/c$. In calculating the geometric constant C, G_0 is G evaluated at $k = 0$. The evaluation point for pressure is $\mathbf{x}$, and subscript 1 denotes quantities at a source position. Note that the convention for the direction of the surface normal is the opposite of that adopted by Wu and Lee [13].

To calculate the scattered field, equation (1) must be solved subject to the appropriate boundary condition and can then be used to calculate the radiated field. The boundary condition for a rigid surface is that the surface normal velocity be zero or, in terms of the incident and scattered fields p_{inc} and p_{sc}, respectively,

$$\frac{\partial p_{sc}}{\partial \mathbf{n}} \equiv -\frac{\partial p_{inc}}{\partial \mathbf{n}}.$$

The incident field will be the field radiated by a source distribution characteristic of a single harmonic of a rotating disc source.

To perform the calculations, the incident and scattered fields are decomposed into azimuthal modes:

$$p = \sum_{m=-\infty}^{\infty} p_m(r, z)\,\mathrm{e}^{\mathrm{j}m\theta}.$$

An incident field can be decomposed into such modes and the sound field of a rotating source consists of one such mode at a harmonic frequency. For this reason, we will consider only single azimuthal modes from now on. Upon assuming that only a single

mode is present and changing to cylindrical co-ordinates, equation (1) becomes

$$C(r,z)p_m(r,z) = \int_\Gamma \left[g_m \frac{\partial p_m}{\partial \mathbf{n}_1} - p_m \frac{\partial g_m}{\partial \mathbf{n}_1} \right] r_1 \, \mathrm{d}\Gamma, \tag{3}$$

where

$$g_m = \int_0^{2\pi} \frac{\mathrm{e}^{\mathrm{j}(kR+m\theta_1)}}{4\pi R} \, \mathrm{d}\theta_1.$$

The main numerical difficulty in solving this integral equation is the isolation and integration of the singularity which appears in g_m as the field point approaches the source position. This can be done in a number of ways but the most convenient is to regularize the integral by subtracting out the singular part and treating it separately. This leads to a quite general expression which can be evaluated in a number of ways and which requires no special assumptions about the duct geometry. The Green function g_m can be rewritten as follows:

$$g_m = g_m^{(\mathrm{b})} + g_m^{(\mathrm{s})}, \qquad g_m^{(\mathrm{b})} = \int_0^{2\pi} \mathrm{e}^{\mathrm{j}m\theta_1} \frac{\mathrm{e}^{\mathrm{j}kR} - 1}{4\pi R} \, \mathrm{d}\theta_1, \tag{4, 5}$$

$$g_m^{(\mathrm{s})} = \int_0^{2\pi} \frac{\mathrm{e}^{\mathrm{j}m\theta_1}}{4\pi R} \, \mathrm{d}\theta_1. \tag{6}$$

In this form, $g_m^{(\mathrm{b})}$ is bounded as $(r,z) \to (r_1, z_1)$ and can be integrated by using standard numerical schemes while the singular part $g_m^{(\mathrm{s})}$ can be evaluated analytically by using recursion relations or asymptotic expansions based on well-understood special functions.

3.1. EVALUATION OF SINGULAR TERMS

The singular part of g_m can be expressed as a generalized elliptic-type integral, a special function which has been extensively studied [14–17] due to its importance in radiation problems. A number of methods have been published for the evaluation of such functions over the full range of useful parameters. $g_m^{(\mathrm{s})}$ can be rewritten as

$$g_m^{(\mathrm{s})} = \frac{1}{4\pi\rho} H(1, m, \lambda), \tag{7}$$

$$H(n, m, \lambda) = \int_0^{2\pi} \frac{\cos 2m\phi}{(1 - \lambda^2 \cos^2 \phi)^{n/2}} \, \mathrm{d}\phi, \tag{8}$$

where

$$\rho^2 = (r + r_1)^2 + (z - z_1)^2$$

and

$$\lambda^2 = \frac{4rr_1}{\rho^2}.$$

Similarly, the derivatives of $g_m^{(\mathrm{s})}$, required for the calculation of $\partial g_m / \partial \mathbf{n}_1$ can be expressed as

$$\frac{\partial g_m^{(\mathrm{s})}}{\partial x} = -\frac{1}{4\pi\rho^2} \frac{\partial \rho}{\partial x} H(1, m, \lambda) + \frac{\lambda}{4\pi\rho} \frac{\partial \lambda}{\partial x} H(3, m, \lambda), \tag{9}$$

where x is either r_1 or z_1. The functions required to evaluate the derivatives of $g_m^{(s)}$ are

$$\frac{\partial \rho}{\partial r_1} = \frac{r + r_1}{\rho}, \quad \frac{\partial \lambda}{\partial r_1} = \frac{\lambda}{2r_1} - \frac{\lambda}{\rho}\frac{\partial \rho}{\partial r_1},$$

$$\frac{\partial \rho}{\partial z_1} = -\frac{z - z_1}{\rho}, \quad \frac{\partial \lambda}{\partial z_1} = -\frac{\lambda}{\rho}\frac{\partial \rho}{\partial z_1}.$$

A number of recursion methods have been given for the evaluation of $g_m^{(s)}$ [18–20] but for high m, it is desirable to use methods which do not risk inaccuracy due to possible instability or loss of precision in the recursion relation. For this reason, the formulae given by Björkberg and Kristensson [21] are used. The function H can be expressed in terms of a hypergeometric series:

$$H(n, m, \lambda) = \frac{\pi}{m!}\left(\frac{n}{2}\right)_m 2^{3-n}\lambda'^{1-n}\lambda^{2m}(1 + \lambda')^{n-2m-2} \times {}_2F_1\left(1 - \frac{n}{2}, 1 + m - \frac{n}{2}; 1 + m; \left(\frac{1 - \lambda'}{1 + \lambda'}\right)^2\right), \tag{10}$$

where $\lambda' = (1 - \lambda^2)^{1/2}$. Direct computation of the series is lengthy when $\lambda \to 1$ and in this case an asymptotic series can be used [21]. For $n = 2n' + 1$ (which covers all of the cases of interest in this study)

$$H(2n' + 1, m, \lambda) = \frac{\lambda^{2m}\lambda'^{1-n}}{(1/2)_{n'}}\left[\sum_{k=0}^{n'-1} (-1)^k C_k (n' - 1'k)!\lambda'^{2k} + \sum_{k=n'}^{\infty} \frac{C_k}{(k - n')!} h_k(\lambda')\lambda'^{2k}\right], \tag{11}$$

where

$$C_k = (\tfrac{1}{2} + m)_k (\tfrac{1}{2} + m - n')_k / k!,$$

$$h_k(\lambda') = \psi(1 + k) + \psi(1 + k - n') - \psi(\tfrac{1}{2} + m + k) - \psi(\tfrac{1}{2} + m - n' + k) - 2\log\lambda'.$$

Here, ψ is the logarithmic derivative of the gamma function and $(a)_n$ is Pochammer's symbol

$$(a)_n = \frac{\Gamma(a + n)}{\Gamma(a)}.$$

These formulae give all the information necessary to evaluate efficiently the singular part of the Green function.

3.2. NUMERICAL IMPLEMENTATION

Equation (3) is solved using a boundary element method. The boundary Γ is discretized using isoparametric elements, as in reference [20]. Each element is discretized using n points and all quantities on the element are then interpolated using the n shape functions N_k, $k = 1, \ldots, n$. The local co-ordinate on the element is η, $0 \leqslant \eta \leqslant 1$ and a quantity f on the element is evaluated by using

$$f = \sum_{k=1}^{n} N_k(\eta) f_k$$

with f_k the value of f at node k. In this study, four-node elements were used with the cubic-shape functions

$$N_1 = \tfrac{1}{2}L_1(3L_1 - 1)(3L_1 - 2), \quad N_2 = \tfrac{1}{2}L_2(3L_2 - 1)(3L_2 - 2),$$

$$N_3 = \tfrac{9}{2}L_1L_2(3L_1 - 1), \quad N_4 = \tfrac{9}{2}L_2L_1(3L_2 - 1),$$

$$L_1 = 1 - \eta, \quad L_2 = \eta.$$

Use of cubic interpolation guarantees smoothness of the surface quantities and of their derivatives.

An important part of a realistic scattering calculation is the treatment of sharp edges on the scattering body. At a sharp edge, the direction of the surface normal changes abruptly and depends on the direction in which the edge is approached. In this work, sharp corners are modelled using double nodes [20]. By placing two nodes at the sharp edge, two different normals can be specified. By making each of the nodes part of the appropriate element, the correct behaviour of the normal can be enforced as the edge is approached from either side (Figure 2).

The integration of the singular part of the Green function must also be considered. A number of approaches have been used in the past, including analytical integration for restricted geometries [12, 22] or for linear surface elements [23]. In this work, a generalized Gaussian quadrature has been used. This is a method which provides base points and weights as for standard Gaussian quadrature but for the integration of functions with singularities of specified form. Algorithms are available for the derivation of base points and weights [24] and coefficients have been published for integration over isoparametric elements of functions containing a logarithmic singularity [25]. The advantages of using such a method in this case are that it can be easily adapted to high order elements, that no restriction is placed on the geometry or on the form of discretization and that no special treatment of the singular functions is required. A further advantage, of use in future work, is that algorithms have recently been published to derive quadrature rules for singular and hypersingular integrals [26]. This means that the hypersingular boundary integral equations required for lined ducts [12] can be solved with identical numerical procedures, only the quadrature coefficients being changed.

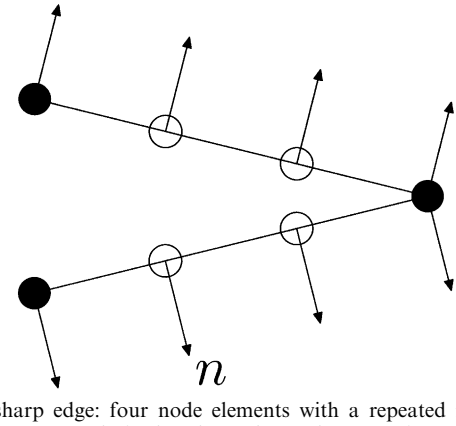

Figure 2. Treatment of a sharp edge: four node elements with a repeated node at the edge. Solid circles represent end points of elements, open circles interior points. The normal n varies smoothly approaching the sharp edge from either side but is discontinuous at the edge.

3.3. SOURCE MODEL

The rotor is modelled as a distributed axial force (acoustic dipole) with azimuthally varying strength:

$$f_z = \mathrm{e}^{\mathrm{j}m\theta}. \tag{12}$$

Standard theory gives an integral for the resulting incident field [5],

$$p_m = \mathrm{e}^{\mathrm{j}m\theta} z \int_0^1 \int_0^{2\pi} \frac{\mathrm{e}^{\mathrm{j}(kR - m\theta_1)}}{4\pi R^3} (1 - \mathrm{j}kR)\, \mathrm{d}\theta_1 r_1\, \mathrm{d}r_1, \tag{13}$$

where lengths have been scaled on disc radius a and $k = mM_t$ where $M_t = \Omega a/c$, the source tip Mach number. The acoustic pressure p_m can be calculated by evaluation of the double integral in equation (13) or by using an alternative method developed for the study of rotor noise fields [4, 5]. A source model of this type is used in preference to point or line source models [12] because of its greater realism. From studies of rotor noise fields, it has been found that a disc source model contains features which are not to be seen in the field around ring sources. In particular, it does not contain singularities in the near field, an important point in calculating the field incident on the duct near the rotor. As is common in ducted source predictions [7], the effect of the duct on the source has been neglected.

4. RESULTS

The scattering calculation method developed in section 3 has been applied to the problem of radiation from a ducted fan with the geometry shown in Figure 3. The duct generator Γ is a Joukowsky section with length and thickness as shown and the rotor placed at the quarter chord. The geometry is held constant while the rotor tip Mach number is varied to examine the effect on the radiated field. Three tip Mach numbers were chosen, $M_t = 0{\cdot}89$, $1{\cdot}1$ and $1{\cdot}5$. The azimuthal order $m = 16$. Figure 3 also shows the co-ordinate system (R, ψ), centred on the intake, which is used to plot the acoustic directivity.

For the specified azimuthal order, the maximum and minimum cut-off Mach numbers (i.e., the cut-off Mach numbers at the minimum and maximum duct internal radius) are $1{\cdot}129$ and $1{\cdot}0035$, respectively. For the $M_t = 0{\cdot}89$ rotor, no mode is cut on at any point; for the $M_t = 1{\cdot}1$ rotor, the first mode is just cut off at the minimum radius and cut on at the maximum radius; for the $M_t = 1{\cdot}5$ rotor, two modes are cut on at the minimum radius and three at the maximum. The resulting acoustic directivities are shown in Figures 4–6. In each case, the magnitude of the radiated pressure $|p|$ is plotted against ψ at fixed R. In the

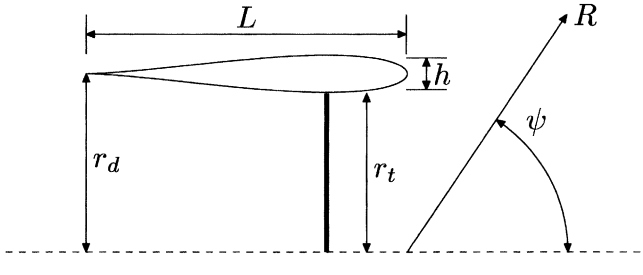

Figure 3. Duct geometry for calculations: $L = 2r_t$, $r_d = 1{\cdot}125r_t$ and $h = L/10$.

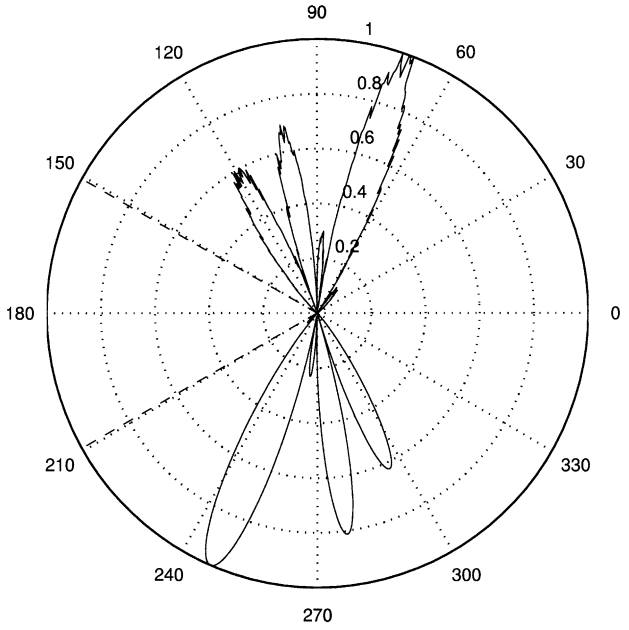

Figure 4. Ducted fan noise directivities, $M_t = 0{\cdot}89$. Upper plot $R = 64$ and lower plot $R = 8$.

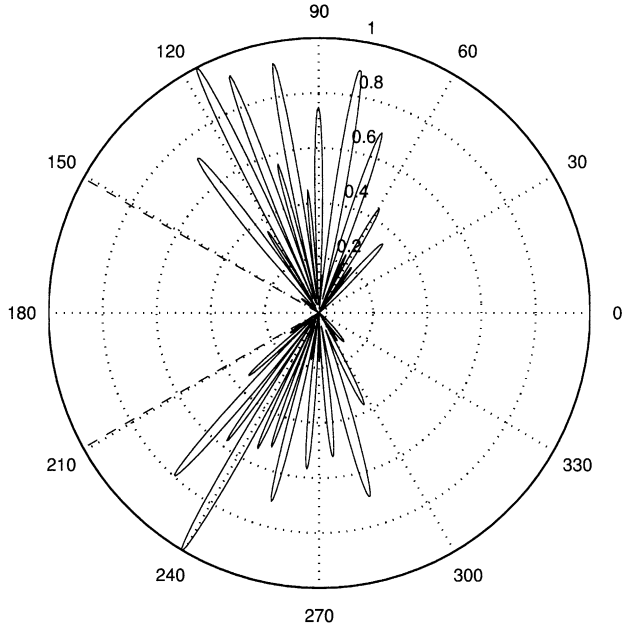

Figure 5. Ducted fan noise directivities, $M_t = 1{\cdot}1$. Upper plot $R = 64$ and lower plot $R = 8$.

upper half of each polar plot $R = 64$ while in the lower half $R = 8$ with length scaled on rotor radius. To ease comparison, the pressures have been scaled on their maximum value at each value of R and, as a reference, a dashed line indicates the angle from the centre of the intake plane to the duct trailing edge. Figure 7 shows the maximum value of pressure as a function of R.

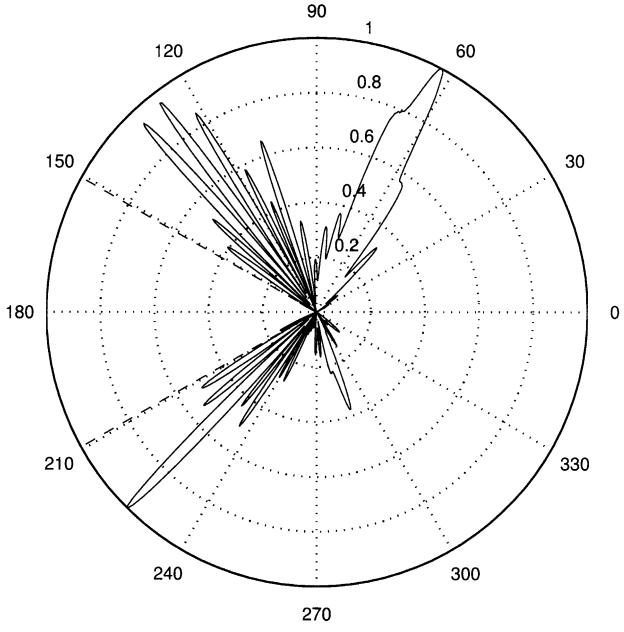

Figure 6. Ducted fan noise directivities, $M_t = 1{\cdot}5$. Upper plot $R = 64$ and lower plot $R = 8$.

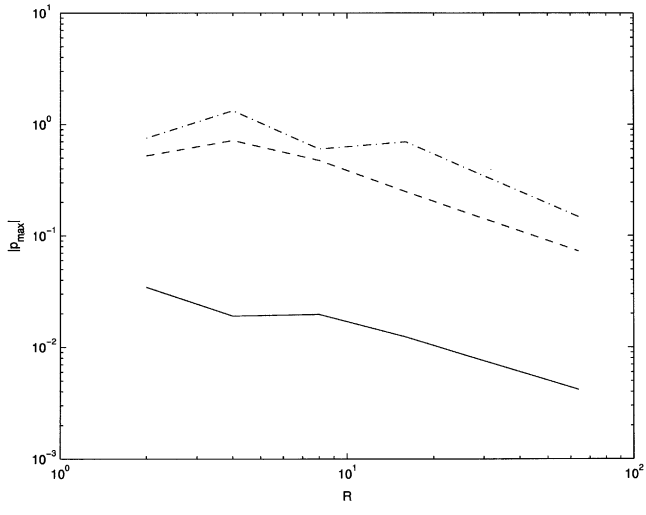

Figure 7. Maximum radiated pressure against R: solid line, $M_t = 0{\cdot}89$; dashed line $M_t = 1{\cdot}1$; dot-dash line $M_t = 1{\cdot}5$.

The maximum value selected for R is greater than the Rayleigh length ka^2 where a is the source radius. For radial separations outside this length, by analogy with the field from a baffled piston [27], a characteristic far field develops. It has been found [28] that the acoustic field in front of the intake plane and behind the exhaust plane is well approximated by a Rayleigh integral so that the Rayleigh distance is a useful parameter. In each of the directivities shown, for $R = 64$ the radial separation $R \sin \psi > ka^2$ when $\psi > 30^\circ$ so that the directivity pattern shown is characteristic of the far field over most of the

range of ψ. In the lower half of the figure, where $R = 8$, the whole range of angle lies in the near field.

Figure 4 shows the directivity of the noise for $M_t = 0{\cdot}89$, a case in which one radial mode is just cut off. It can be seen from this figure that there is some radiation, with a lobe ahead of the intake plane in the far field ($R = 64$) but reference to Figure 7 will show that the absolute level is quite low. It is also clear that there is very little radiation from the exhaust plane, probably because the source is further from the exhaust than from the intake and so any mode is very strongly attenuated by the time it reaches the exhaust. The mode propagating towards the intake is below cut-off but enough energy is transmitted to generate a measurable amount of noise.

When $M_t = 1{\cdot}1$, Figure 5, the first radial mode is cut off at the source plane but cut on at the intake and exhaust. The radiated noise is thus much stronger, as seen in Figure 7, but still comparatively weak behind the exhaust. The complex multilobed radiation pattern behind the intake plane, $\psi > 90^\circ$ is mainly due to interference between the intake and exhaust plane sources and to radiation from the duct side walls.

Finally, when $M_t = 1{\cdot}5$, two modes are cut on at the source plane, and three at the intake and exhaust. This results in stronger radiation both in front of and behind the duct, with one strong lobe in the far field ahead of the intake and a complex interference pattern near the trailing edge. The lobe is also visible in the near field, but is less noticeable due to the scaling on maximum pressure.

The plot of maximum radiated pressure, Figure 7, shows the effect of varying the source frequency. The $M_t = 0{\cdot}89$ data are an order of magnitude lower than for the higher tip Mach numbers. The modes generated by the source are incapable of propagating strongly and are highly attenuated at the duct exit, thus radiating little noise to the far field. The supersonic rotor pressures, however, are quite close, despite the difference in tip Mach number. This is probably due to the fact that the presence or absence of propagating modes is more important than the relative strengths of the sources. If propagating modes are present, there will be strong radiation into the far field, while if all modes are cut off, only a weak radiated pressure field is possible. The similarity in level, though not directivity, between the two supersonic rotor cases is due to the fact that the two sources generate propagating modes.

5. CONCLUSIONS

A boundary element method for scattering by axisymmetric bodies has been developed and applied to the problem of radiation by a ducted rotor. The method used is a standard Helmholtz integral technique with recently developed methods in Gaussian quadrature and the theory of generalized elliptic integrals used to simplify the implementation. In conjunction with a previously developed rotor noise model [4, 5], the radiated field of a ducted rotor at a number of tip Mach numbers has been calculated. It was found that the essential features of the radiated field were captured and that the relationship between the rotor and modal cut-off Mach numbers was as expected. It was also observed that the duct intake radiation can be viewed as that due to a disc source distributed over the intake, giving results similar to those seen in open rotor noise studies.

The obvious, and essential, extension of the work presented here is to the study of noise from ducted rotors in forward flight. If such a study is to be carried out by using a boundary element method, the methods and analysis developed in this paper will be useful. A possible approach to the problem of noise generation will be to treat the problem from

an integrated aerodynamic and acoustic point of view [29, 30] in order to treat the effect of non-uniform flow and of the duct wake on the noise field.

REFERENCES

1. A. Filippone 2000 *Progress in Aerospace Sciences* **36**, 629–654. Data and performances of selected aircraft and rotorcraft.
2. M. J. Lighthill 1952 *Proceedings of the Royal Society of London A* **211**, 564–587. On sound generated aerodynamically. Part I. General theory.
3. J. M. Tyler and T. G. Sofrin 1962 *Transactions of the Society of Automotive Engineers* **70**, 309–332. Axial flow compressor noise studies.
4. C. J. Chapman 1993 *Proceedings of the Royal Society of London A* **440**, 257–271. The structure of rotating sound fields.
5. M. Carley 1999 *Journal of Sound and Vibration* **225**, 353–374. Sound radiation from propellers in forward flight.
6. A. J. Burton and G. F. Miller 1971 *Proceedings of the Royal Society of London A* **323**, 201–210. The application of integral equation methods to the numerical solution of some exterior boundary-value problems.
7. W. Eversman 1995 in *Aeroacoustics of Flight Vehicles* (H. H. Hubbard, editor). Acoustical Society of America. Theoretical models for duct acoustic propagation and radiation.
8. A. H. Nayfeh and D. P. Telionis 1973 *Journal of the Acoustical Society of America* **54**, 1654–1661. Acoustic propagation in ducts with varying cross sections.
9. M. Carley 2000 *Journal of Sound and Vibration* **233**, 255–277. Propeller noise fields.
10. P. R. Prentice 1993 *Proceedings of the Royal Society of London A* **441**, 83–96. Energy transport in rotating sound fields.
11. P. R. Prentice 1992 *Proceedings of the Royal Society of London A* **437**, 629–644. The acoustic ring source and its application to propeller acoustics.
12. M. H. Dunn, J. Tweed and F. Farassat 1999 *Journal of Sound and Vibration* **227**, 1019–1048. The application of a boundary integral equation method to the prediction of ducted fan engine noise.
13. T. W. Wu and L. Lee 1994 *Journal of Sound and Vibration* **175**, 51–63. A direct boundary integral formulation for acoustic radiation in a subsonic uniform flow.
14. L. F. Epstein and J. H. Hubbell 1963 *Journal of Research of the National Bureau of Standards B* **67**, 1–17. Evaluation of a generalized elliptic-type integral.
15. H. M. Srivastava and S. Bromberg 1995 *Mathematical and Computer Modelling* **21**, 29–38. Some families of generalized elliptic-type integrals.
16. S. L. Kalla and V. K. Tuan 1996 *Computers and Mathematics with Applications* **32**, 49–55. Asymptotic formulas for generalized elliptic-type integrals.
17. A. Al-Zamel, V. K. Tuan and S. L. Kalla 2000 *Applied Mathematics and Computation* **114**, 13–25. Generalized elliptic-type integrals and asymptotic formulas.
18. S. D. Gedney and R. Mittra 1990 *IEEE Transactions on Antennas and Propagation* **38**, 313–322. The use of the FFT for the efficient solution of the problem of electromagnetic scattering by a body of revolution.
19. H. S. Kim, J. S. Kim and H. J. Kang 1993 *Journal of Sound and Vibration* **163**, 385–396. Acoustic wave scattering from axisymmetric bodies.
20. W. Wang, N. Atalla and J. Nicolas 1997 *Journal of the Acoustical Society of America* **101**, 1468–1478. A boundary integral approach for acoustic radiation of axisymmetric bodies with arbitrary boundary conditions valid for all wave numbers.
21. J. Björkberg and G. Kristensson 1987 *Canadian Journal of Physics* **65**, 723–734. Electromagnetic scattering by a perfectly conducting elliptic disc.
22. M. H. Dunn, J. Tweed and F. Farassat 1996 in 2*nd AIAA/CEAS Aeroacoustics Conference*, AIAA-96-1770. The prediction of ducted fan engine noise via a boundary integral equation method.
23. T. W. Dawson 1995 *Applied Mathematical Modelling* **19**, 590–599. On the singularity of the axially symmetric Helmholtz Green's function, with application to BEM.
24. J. Ma, V. Rokhlin and S. Wandzura 1996 *SIAM Journal of Numerical Analysis* **33**, 971–996. Generalized Gaussian quadrature rules for systems of arbitrary functions.
25. R. N. L. Smith 2000 *Engineering Analysis with Boundary Elements* **24**, 161–167. Direct Gauss quadrature formulae for logarithmic singularities on isoparametric elements.

26. P. KOLM and V. ROKHLIN 2001 *Computers and Mathematics with Applications* **41**, 327–352. Numerical quadratures for singular and hypersingular integrals.
27. A. D. PIERCE 1989 *Acoustics: An Introduction to its Physical Principles and Applications*. Acoustical Society of America.
28. J. W. POSEY, M. H. DUNN and F. FARASSAT 1998 in 4*th AIAA/CEAS Aeroacoustics Conference*, AIAA 98–2248. Quantification of inlet impedance concept and a study of the Rayleigh formula for noise radiation from ducted fan engines.
29. A. A. MASLOV 1997 *Acoustical Physics* **43**, 179–185. Simultaneous evaluation of the aerodynamic characteristics and sound field of a ducted propeller.
30. M. GENNARETTI, L. LUCERI and L. MORINO 1997 *Journal of Sound and Vibration* **200**, 467–489. A unified boundary integral methodology for aerodynamics and aeroacoustics of rotors.